AFRL-OSR-VA-TR-2013-0468

DYMAFLEX DYNAMIC MANIPULATION FLIGHT EXPERIMENT

DAVID AKIN

UNIVERSITY OF MARYLAND COLLEGE PARK

09/03/2013
Final Report

AIR FORCE RESEARCH LABORATORY
AF OFFICE OF SCIENTIFIC RESEARCH (AFOSR)/RSE
ARLINGTON, VIRGINIA 22203
AIR FORCE MATERIEL COMMAND

REPORT DOCUMENTATION PAGE

Form Approved
OMB No. 0704-0188

1. REPORT DATE *(DD-MM-YYYY)*	**2. REPORT TYPE**	**3. DATES COVERED** *(From - To)*
14-08-2013	Final Report	

4. TITLE AND SUBTITLE

DYMAFLEX: DYnamic MAnipulation FLight EXperiment

5a. CONTRACT NUMBER

5b. GRANT NUMBER

FA9550-11-1-0046

5c. PROGRAM ELEMENT NUMBER

6. AUTHOR(S)

David L. Akin, Katherine McBryan, Nicholas Limparis

5d. PROJECT NUMBER

5e. TASK NUMBER

5f. WORK UNIT NUMBER

7. PERFORMING ORGANIZATION NAME(S) AND ADDRESS(ES)

University of Maryland Space Systems Laboratory
382 Technology Drive
College Park, MD 20742

8. PERFORMING ORGANIZATION REPORT NUMBER

9. SPONSORING / MONITORING AGENCY NAME(S) AND ADDRESS(ES)

10. SPONSOR/MONITOR'S ACRONYM(S)

11. SPONSOR/MONITOR'S REPORT NUMBER(S)

12. DISTRIBUTION / AVAILABILITY STATEMENT

public release

13. SUPPLEMENTARY NOTES

14. ABSTRACT

The DYnamic MAnipulation FLight EXperiment (DYMAFLEX) is intended to perform basic research on the dynamic interactions between high-rate motions of a manipulator on a free-flying spacecraft bus. The DYMAFLEX spacecraft consists of a 50-kg small satellite incorporating a cold-gas reaction control system for attitude control, which carries an 80-cm four degree-of-freedom manipulator with accommodations for the addition of various sized tip masses for changing dynamic properties on-orbit. The successful flight of DYMAFLEX would accomplish the flight validation of all critical technologies for smallsat-based satellite servicing capabilities

15. SUBJECT TERMS

16. SECURITY CLASSIFICATION OF:			**17. LIMITATION OF ABSTRACT**	**18. NUMBER OF PAGES**	**19a. NAME OF RESPONSIBLE PERSON**
a. REPORT	**b. ABSTRACT**	**c. THIS PAGE**			**19b. TELEPHONE NUMBER** *(include area code)*

SPACE MANIPULATOR CONTROL FOR THE DYMAFLEX FLIGHT EXPERIMENT

Mr. Nicholas D'Amore
University of Maryland, College Park, United States, ndamore@umd.edu

Dr. David L. Akin*

Unlike traditional fixed-base manipulators, manipulators used in space are mounted to a spacecraft which may move freely in response to any forces or torques. This results in a highly coupled dynamical system. In the past, robotic arms have often been slow and lightweight in comparison to their host spacecraft; but as economic incentives drive the development of smaller, faster, lighter vehicles, this coupling will present an increasing challenge in the development of suitable control systems. To improve understanding of the dynamics of this coupled system and to demonstrate and validate proposed controllers in the space environment, the University of Maryland Space Systems Lab is constructing the DYnamic MAnipulation FLight EXperiment (DYMAFLEX) microsatellite, the development of which is partially funded by the United States Air Force University Nanosat Program. Equipped with a high-performance manipulator representing approximately 14% of the mass of the combined system and having greater rotational inertia at full extension than the spacecraft itself, the DYMAFLEX vehicle represents the ideal test bed for space manipulator dynamics and control. This paper presents an overview of space manipulator control as it relates to the DYMAFLEX science mission, with simulation results exploring an intended maneuver in Cartesian space. The mission is designed to provide empirical validation of existing models for the behavior of a space manipulator as well as to provide a basis for comparison between proposed control strategies to assess their strengths and weaknesses in the actual application environment. In this paper, a simple Transpose Jacobian controller is compared to more sophisticated approaches, including the Modified Transpose Jacobian controller of Papadopoulos and Moosavian. A technique is proposed for mitigating the chattering problem associated with the MTJ strategy. The effect of measurement noise is explored. An adaptive controller is considered as a further means of improving performance. Preliminary conclusions are drawn, to be verified on the DYMAFLEX platform.

I. INTRODUCTION

Manipulators used in space are mounted to a spacecraft which may move freely in response to any forces or torques, resulting in highly coupled dynamical behavior not seen in traditional, fixed-base robotics. Historically, robotic arms have often been slow and lightweight in comparison to their host spacecraft; but as economic incentives drive the development of smaller, faster, lighter vehicles, this coupling will present an increasing challenge in the development of suitable control systems. In return, such systems will open up increasingly favorable opportunities in satellite servicing—repairing or replacing failed components rather than launching entirely new satellites, or harvesting functional parts from defunct satellites to assemble useful systems from what would otherwise join the countless orbital debris already circling our planet. Moreover, many near-Earth objects have such low gravity that a precision sampling mission would be very much an exercise in free-flying manipulation. Such missions would help to characterize the threat these objects pose to the Earth and to improve our geological understanding of the solar system, placing our understanding of the Earth's geology in its larger context.

Ground-based testing does not readily lend itself to the evaluation of space manipulator systems. Parabolic flight to create short-term microgravity does not permit enough experiment time to explore extended maneuvers or disturbance recovery. Hydrodynamic drag may overwhelm important components of the system response in neutral buoyancy. Planar air-bearing vehicles do not exhibit the full dynamic response of 3D motion. To improve understanding of the dynamics of this coupled system and to demonstrate and validate proposed controllers in the space environment, the University of Maryland Space Systems Laboratory is therefore constructing the DYnamic MAnipulation FLight EXperiment (DYMAFLEX) microsatellite, the development of which is partially funded by the United States Air Force University Nanosat Pro-

*University of Maryland, College Park, United States, dakin@ssl.umd.edu

gram (UNP). Equipped with a high-performance manipulator representing approximately 14% of the mass of the combined system and having greater rotational inertia at full extension than the spacecraft itself, the DYMAFLEX vehicle represents the ideal test bed for space manipulator dynamics and control.

I.I The DYMAFLEX vehicle

The DYMAFLEX vehicle is shown in Figure 1. Developed in the university environment, both undergraduate and graduate students are involved in all aspects of the design process. It consists of a 7 kg, 4 degree-of-freedom (DOF) roll-pitch-roll-pitch robotic manipulator mounted to a 43 kg microsatellite measuring approximately 45 × 45 × 40 cm. This high-performance manipulator is 70 cm long and is equipped with an interchangeable tip mass to allow for variation of the system inertial properties during the course of the mission. Even without any tip mass in place, the arm has a rotational inertia about its shoulder of approximately 1.1 kg-m^2 at full extension, 10% greater than that of the main spacecraft body about its center of mass. The vehicle bus is equipped with 16 cold-gas CO_2 thrusters for full 6-DOF position and attitude control. As a participant in the UNP, DYMAFLEX will be competitively considered for launch as a secondary payload. For more detail on the DYMAFLEX project, including a description of the planned experimental maneuvers, see Reference 1.

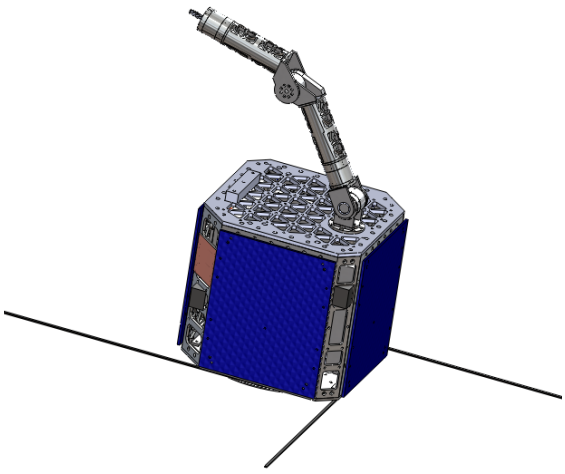

Figure 1: DYMAFLEX vehicle with arm and antennas deployed

II. EQUATIONS OF MOTION

Papadopoulos [2] derives the equations of motion of a space manipulator, showing their top-level, matrix-vector representation to be of identical form to those of a fixed-base manipulator, albeit with much more complicated expressions contained within each term. The top-level form is given by:

$$\mathbf{M}(\underline{\theta})\dot{\underline{\nu}} + \underline{C}(\underline{q}, \underline{\nu}) = \underline{u}$$

where $\mathbf{M}$ is the system inertia matrix, $\underline{q}$ is the position state vector (consisting of the manipulator joint angles $\underline{\theta}$, spacecraft attitude quaternion, and spacecraft center of mass location[†]), $\underline{\nu}$ is the system velocity state, $\underline{u}$ is the vector of control inputs, and $\underline{C}$ is the vector of nonlinear acceleration terms. Because the equations of motion are structurally identical to those of a fixed-base manipulator, it is recognized that virtually any control scheme developed for use on a fixed-base manipulator is theoretically applicable to a space manipulator as well, perhaps with additional sensing requirements and greater sensitivity to uncertainty in the system parameters. Although Papadopoulos's primarily Lagrangian derivation of the system dynamics leads to some useful theoretical conclusions, a Newtonian approach [3] was found to be more conducive to practical numerical simulation because its implementation does not require taking derivatives of lengthy symbolic expressions.

As in the case of a fixed-base manipulator, the equations of motion are most readily written in joint space (as above), whereas the task is more often defined in Cartesian space. A Jacobian matrix can be used to map velocities between the two spaces according to $\dot{\underline{r}}_T = \mathbf{J}\underline{\nu}$, where $\underline{r}_T$ is the end effector tip position and $\mathbf{J}$ is the Jacobian matrix. Papadopoulos [2] presents the space manipulator Jacobian for both the free-flying case, in which the spacecraft is actuated by means of thrusters, as well as the free-floating case, in which the spacecraft passively reacts to disturbances from the arm. It is noteworthy here that, unlike the case of a fixed-base manipulator, the Jacobian of a space manipulator is a function of inertial parameters in addition to geometric properties, thus exacerbating the difficulties posed by any uncertainty in the system parameters. Again as in the case of a fixed-base manipulator, the transpose of the Jacobian matrix can be used to convert a static Cartesian force/torque

[†]Papadopoulos uses instead the center of mass of the combined spacecraft-manipulator system, which results in less complicated expressions but is not as useful for controls purposes.

at the end effector into a joint space torque vector[‡].

Moosavian and Papadopoulos [4] convert the equations of motion into Cartesian space under the assumption that the Jacobian matrix is square and invertible:

$$\mathbf{M}(\underline{\theta})\dot{\underline{\nu}} + \underline{C}(\underline{q},\underline{\nu}) = \underline{u} \rightarrow \mathbf{M}_x(\underline{\theta})\ddot{\underline{r}}_T + \underline{C}_x(\underline{q},\underline{\nu}) = \underline{F}$$

where

$$\mathbf{M}_x = \mathbf{J}^{-T}\mathbf{M}\mathbf{J}^{-1}$$
$$\underline{C}_x = \mathbf{J}^{-T}\underline{C} - \mathbf{M}_x\dot{\mathbf{J}}\underline{\nu}$$
$$\underline{F} = \mathbf{J}^{-T}\underline{u}$$

This assumption of a square and invertible Jacobian is somewhat troubling in the case of a free-flying space manipulator, for which the spacecraft thrusters provide six degrees of freedom and the presence of any arm at all is redundant. The effect of this assumption on their resulting stability analysis is discussed briefly in the next section.

III. CONTROL STRATEGIES

This section describes several control strategies considered for the task space control of a space manipulator.

III.I Transpose Jacobian (TJ)

The Cartesian representation of the system dynamics presented in the previous section motivates the definition of a control law directly in Cartesian space:

$$\underline{F} = \mathbf{K}_p\underline{e} + \mathbf{K}_d\dot{\underline{e}}$$

where $\underline{e} = \underline{r}_{T,des} - \underline{r}_T$ and $\mathbf{K}_p$ and $\mathbf{K}_d$ are positive definite gain matrices. The control input therefore takes the form of the Transpose Jacobian (TJ) controller:

$$\underline{u} = \mathbf{J}^T\underline{F} = \mathbf{J}^T(\mathbf{K}_p\underline{e} + \mathbf{K}_d\dot{\underline{e}})$$

Moosavian and Papadopoulos [4] present a stability analysis based upon the Cartesian-space formulation of the system dynamics presented in the previous section. It is worth noting here that the authors' assumption of a square Jacobian can actually be relaxed somewhat without entirely invalidating their stability analysis. Outside of singular configurations, the problem is one of non-uniqueness rather than non-existence of the Jacobian's inverse. By instead augmenting the 6-DOF Cartesian space with N additional variables (the joint angles, for example), the Jacobian mapping into this new augmented task space becomes a square matrix. Setting the newly-inserted elements of $\mathbf{K}_p$ and $\mathbf{K}_d$ to zero so as not to modify the system behavior, the authors' original proof demonstrates Lyapunov stability even in the case of a redundant manipulator, so long as this augmented Jacobian does not become singular.

III.II Modified Transpose Jacobian (MTJ)

Because the TJ control strategy employs no knowledge of the system dynamics and depends on large gains to overwhelm such dynamics, it stands to reason that a more considered choice of control law could reduce tracking error and/or exerted control effort by making use of such knowledge. Returning to the TJ control law, Moosavian and Papadopoulos consider inserting an additional term $\underline{h}$ into the expression for $\underline{F}$, yielding:

$$\mathbf{M}_x\ddot{\underline{r}}_T + \underline{C}_x = \mathbf{K}_p\underline{e} + \mathbf{K}_d\dot{\underline{e}} + \underline{h}$$

Ideally, one might choose $\underline{h} = \mathbf{M}_x\ddot{\underline{r}}_T + \underline{C}_x$ so as to cancel out the terms on the left hand side and produce a linear system for which even small gains would guarantee asymptotic convergence. Doing so, however, requires exact knowledge of the system dynamics. Computing these terms can be computationally demanding even when the system parameters are known perfectly, and adaptively learning any parameters which may not be known a priori adds a further level of complexity.

In an attempt to mimic some of the advantages of adaptive control while avoiding the associated computational complexity, the authors [4] propose reusing the control effort exerted at the previous controller update cycle, $\underline{F}_{t-\Delta t}$. If the system states are changing slowly enough, $\mathbf{M}_x\ddot{\underline{r}}_T + \underline{C}_x = \underline{F}$ suggests that $\mathbf{M}_x\ddot{\underline{r}}_T + \underline{C}_x \approx \underline{F}_{t-\Delta t}$ and one might expect the choice $\underline{h} = k\underline{F}_{t-\Delta t}$ to approximate the desired behavior. This gives rise to the Modified Transpose Jacobian (MTJ) controller:

$$\underline{u} = \mathbf{J}^T(\mathbf{K}_p\underline{e} + \mathbf{K}_d\dot{\underline{e}} + k\underline{F}_{t-\Delta t})$$

To avoid excessive force/torque commands, the reg-

[‡] "Joint space" refers here to the space of the position state $\underline{q}$, which includes not only joint angles but also the spacecraft location and attitude; this "torque vector" therefore includes the translational force of the thruster system.

ulating factor k is chosen as:

$$k = \exp\left(-\frac{\|\underline{e}\|}{\varepsilon_0} - \frac{\|\underline{\dot{e}}\|}{\varepsilon_1}\right)$$

where ε_0 and ε_1 are scaling constants.

III.III Filtered Modified Transpose Jacobian (FMTJ)

It is a known shortcoming of the MTJ controller that it can result in a high-frequency chattering of the control input $\underline{u}$, thus requiring higher-bandwidth actuation, increasing wear and tear on the actuators, and possibly exciting flexible modes or other unmodeled dynamics. Karimi and Moosavian have presented a technique for mitigating this problem, but only in the case of repetitive motion commands [5]. Instead, it is proposed here to low pass filter the $\underline{h} = k\underline{F}_{t-\Delta t}$ term which the MTJ strategy inserts into the basic TJ control law according to the following formula:

$$\underline{h}_i = \underline{h}_{i-1} + k_f(k\underline{F}_{i-1} - \underline{h}_{i-1})$$

where $k_f < 1$. The proportional and differential terms remain unmodified and may still respond to high-bandwidth content in the desired trajectory, but the $\underline{h}$ term which was responsible for the unwanted chattering is now forced to vary more slowly.

III.IV Inverse Dynamics (ID)

In the case where the system dynamics are perfectly known and sufficient computational capacity is available, the predicted system behavior may be fed forward to linearize the system [6]. Choosing the control input as:

$$\underline{u} = \mathbf{M}\underline{\dot{\nu}}_{ref} + \underline{C}$$

where $\underline{\dot{\nu}}_{ref}$ is a reference *acceleration* in joint space results in a linearized system for which $\underline{\dot{\nu}} = \underline{\dot{\nu}}_{ref}$. In order to convert this into the task space, a pseudoinverse of the Jacobian may be used:

$$\underline{\dot{\nu}}_{ref} = \mathbf{J}^{\dagger}(\underline{\ddot{x}}_{ref} - \dot{\mathbf{J}}\underline{\nu})$$

Note that this requires not only the manipulator Jacobian (as in the case of previous control schemes), but also the time derivative of the Jacobian, the system inertia matrix $\mathbf{M}$, and the velocity-squared terms $\underline{C}$. In exchange for this computational complexity, the system is reduced to the double integrator $\underline{\ddot{r}}_T = \underline{\ddot{x}}_{ref}$, and $\underline{\ddot{x}}_{ref}$ may be chosen as:

$$\underline{\ddot{x}}_{ref} = \underline{\ddot{r}}_{T,des} + K_d\underline{\dot{e}} + K_p\underline{e}$$

IV. COMPARISON OF PERFORMANCE

IV.I Basis of Comparison

As a preliminary comparison of the above-described controllers, each was evaluated in a test maneuver consisting of motion of the end effector at a nominal speed of 5 cm/s along a circle in inertial space, given by the following equation (in meters):

$$\underline{x}_{des} = \begin{pmatrix} -0.0674 \\ 0 \\ 0.5066 \end{pmatrix} + 0.1 \begin{pmatrix} \sin(0.5t) \\ 0 \\ \cos(0.5t) \end{pmatrix}$$

with the shoulder of the vehicle initially at the origin of the inertial frame and initial joint angles $\underline{\theta}_0 = [\ 0 \quad \pi - \frac{1}{2} \quad 0 \quad 0\ ]^T$. The system begins at rest, introducing an initial velocity error for which the controller must compensate. Figure 2 shows this path relative to the DYMAFLEX vehicle in its initial orientation. The free-flying form of the Jacobian is used here, and spacecraft thrusters are therefore employed in addition to the manipulator joint degrees of freedom. The controllers were implemented at an update rate of 100 Hz.

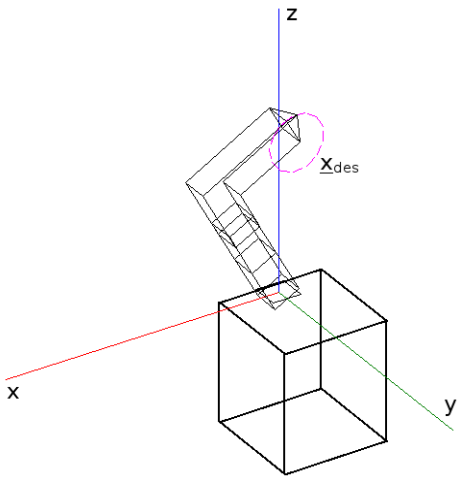

Figure 2: Desired trajectory relative to initial system pose

The following cost function was defined in order to quantify the performance of each controller:

$$\phi_{\text{track}} = 10^3 \sum_i \underline{e}_i^T \underline{e}_i$$

$$\phi_{\text{effort}} = \sum_i \underline{u}_i^T \underline{u}_i$$

$$\Phi = \phi_{\text{track}} + \phi_{\text{effort}}$$

where the index i counts through each of the controller update cycles. The composite cost function Φ represents a combination of the tracking error and control effort exerted throughout the test maneuver, and the factor of 10^3 was inserted so that the two contributing terms would be of comparable magnitude. For the present discussion, units are discarded in the evaluation of this cost metric. The tracking error vector $\underline{e}$ is expressed in meters; and the control input $\underline{u}$ is a mixture of Newtons and Newton-meters. More sophisticated analyses might give more consideration to the relative weightings, perhaps penalizing use of thruster propellant more heavily than use of the arm's electrical actuators.

Smaller values of Φ represent better performance in the trade-off between control effort and tracking performance. The gains employed by each controller were optimized via the Nelder-Mead simplex search method (as implemented in the MATLAB function `fminsearch`) in order to minimize the above cost function. Although this is not a rigorous optimization and no guarantee of convergence to the global minimum is available, it is presented here as an effort to tune each of the controllers for as fair a comparison as is reasonably achievable. For simplicity, all gains were limited to scalar quantities.

IV.II Results

Table 1 presents the final optimized gains selected for each of the controllers, with the corresponding cost value Φ corresponding to one cycle of the circular path given in Table 2. The TJ strategy employs larger gains than the MTJ and FMTJ cases, which took similar parameter choices to one another. For the FMTJ strategy, k_f was chosen as 0.3 and was not optimized.

Most notably, the score of the ID control scheme was orders of magnitude worse than any of the others considered in this study. Clearly, since the error dynamics have been linearized, an arbitrarily small tracking cost ϕ_{track} could be theoretically achieved through the use of large gains. However, the effort of forcing the system to behave linearly (a condition which the other controllers do not attempt to enforce) has overwhelmed any such savings and driven the optimization to select very small gains. That the MTJ strategy exercised its control effort so much more efficiently than the ID scheme calls into question the intuition which led to the MTJ design, which was intended to approximately linearize the system. However, in this simulation the system depended heavily upon the thrusters to translate the entire system while the arm moved very little. Use of a different Jacobian pseudoinverse (the Moore-Penrose pseudoinverse was employed here) might improve this situation.

	K_p	K_d	ϵ_0	ϵ_1
TJ	56.71	16.40	n/a	n/a
MTJ	21.72	12.40	0.0091	0.0238
FMTJ	23.68	13.22	0.0081	0.0196
ID	0.744	1.647	n/a	n/a

Table 1: Optimized gains

	ϕ_{effort}	ϕ_{track}	Φ
TJ	37.14	5.39	42.53
MTJ	31.72	5.09	36.81
FMTJ	31.81	5.03	36.83
ID	1434	94.61	1528

Table 2: Controller performance

On the basis of its Φ score alone, the MTJ scheme appears to have performed quite well, improving its score by approximately 13% versus the basic TJ scheme without requiring any heavy computation or imposing additional sensing requirements. However, as shown in Figure 3, the control signal begins chattering quite appreciably after approximately 11 seconds, as the system begins to spend more and more time within the error band specified by ϵ_0 and ϵ_1. As seen in Figure 4, however, the FMTJ avoids this chattering with no appreciable decline in performance. This initial result is promising, however a rigorous stability analysis remains for future work.

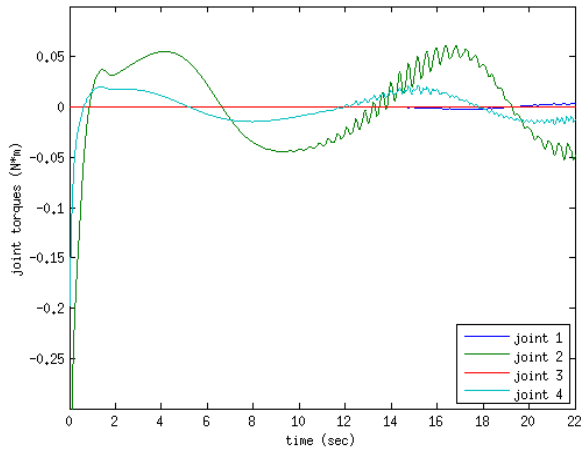

Figure 3: Joint torques commanded by the MTJ controller. Thruster forces and torques exhibited similar chattering.

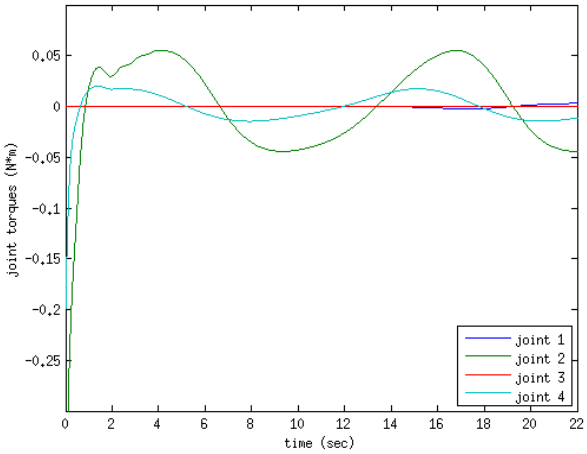

Figure 4: Joint torques commanded by the FMTJ controller.

V. ROBUSTNESS TO NOISE

Error in the system state knowledge is expected to negatively affect system performance in practice. The DYMAFLEX vehicle is not equipped with any means of precision position or attitude determination. For maneuvers expressed in joint space or in a vehicle-fixed coordinate frame, this information is not necessary. For an inertially-defined maneuver such as the one considered in the present study, it will be necessary to integrate readings from the inertial measurement units to approximate this information in order to generate errors $\underline{e}$ and $\dot{\underline{e}}$ for evaluation of the control laws. Although such integration will result in a gradual drift in the estimate of inertial position and attitude, these are ignorable variables in the system dynamics (i.e., they do not appear in the equations of motion which dictate $\dot{\underline{\nu}}$). The effect is equivalent to tracking a target whose inertial position is subject to perturbations, and the use of this fictitious quasi-inertial frame is not expected to fundamentally alter the system behavior versus the true inertial case. In all operational modes, then, errors in the joint angles and rates are of primary concern.

Normally-distributed pseudorandom noise was injected into the controllers' knowledge of the robot joint angles; and joint rate knowledge was generated from finite differencing of these noisy measurements. The noise had zero bias and a standard deviation of 0.15°. To facilitate direct comparison, each controller was subjected to the same noise history as an additive perturbation to the actual joint angles (e.g., at t = 1.00 seconds, all controllers believed the joint 1 angle to be 0.136° larger than the actual value, whatever it was at that point in the simulation). The maneuver of the previous section was repeated using the same gains without any modification to accommodate the noisy signal. Table 3 shows the resulting cost values. Tracking performance degradation was relatively modest for the basic TJ controller, and more pronounced for the more sophisticated techniques. Most notably, however, the control effort metric ϕ_{effort} for all controllers increased by orders of magnitude. This has serious implications in terms of energy usage and required actuator performance.

	ϕ_{effort}	ϕ_{track}	Φ
TJ	4.1×10^4	5.64	4.1×10^4
MTJ	2.3×10^4	30.29	2.3×10^4
FMTJ	2.6×10^4	25.38	2.6×10^4
ID	7.7×10^5	4.6×10^4	8.2×10^5

Table 3: Controller performance without noise mitigation

Clearly, use of raw joint angle measurements will not be adequate in the presence of this level of noise. The simulations were therefore repeated with both the angle and rate values subjected to the same low pass filter as given for $\underline{h}$ in the FMTJ strategy, with $k_f = 0.2$. Interestingly, although the MTJ strategy was expected to have superior noise rejection capabilities due to its use of smaller gains, the unmodified TJ approach yielded superior tracking performance while exerting less control effort. Although the FMTJ strategy also yielded inferior

tracking performance as compared to TJ, it did so while exerting substantially less control effort than either of those two strategies, thus yielding a superior combined score for the relative weights for which it was tuned. As in all previous trials, the ID controller yielded the worst performance, however it experienced the smallest percent degradation due to the presence of noise, achieving essentially the same tracking score with only a 25% increase in control effort cost versus the noise-free case. This is to be expected, however, given the very small gains used here.

	ϕ_{effort}	ϕ_{track}	Φ
TJ	159.6	8.43	168.1
MTJ	188.4	10.46	198.9
FMTJ	145.8	10.56	156.4
ID	1793	93.53	1886

Table 4: Controller performance with low pass filtered angle and rate data

What is again not evidenced in the cost metric Φ is high frequency oscillation in the control input $\underline{u}$. Figure 5 shows a close look at the first five seconds of this maneuver for the FMTJ controller (itself a slight improvement over the MTJ case). These sharp and high-speed fluctuations in the control signal are extremely problematic. The ID controller, as shown in Figure 6, exhibited appreciably less oscillation than the other other controllers. This is again undoubtedly due to the use of small gains and is of little value given the resulting poor performance in terms of control effort and tracking error.

Joint angle sensing is the subject of an ongoing trade study. Although 0.15° is the expected error if the DYMAFLEX system relies on motor commutation for its positional knowledge, it is estimated that absolute encoders would allow for joint angle knowledge to within 0.038°. Rescaling the same noise history to have a standard deviation of 0.038°, with the values filtered as before, resulted in the performance metrics shown in Table 5. Although the FMTJ again yields an improvement over the MTJ technique, the basic TJ with its larger gains is more successful in overwhelming the effect of the errors, reversing our conclusion from the idealized cases of the previous section. Figures 7 and 8 show the joint torques commanded by the TJ and FMTJ controllers, respectively. It can be seen that the joint 3 torque in the FMTJ case oscillates at approximately 2 Hz with a magnitude of approximately 0.1 N-m, whereas the TJ signal is considerably more benign. The MTJ case, not shown, is very similar to the FMTJ case but slightly larger in magnitude. Improving the filtering of joint rate values to reduce this oscillation will be the subject of future work.

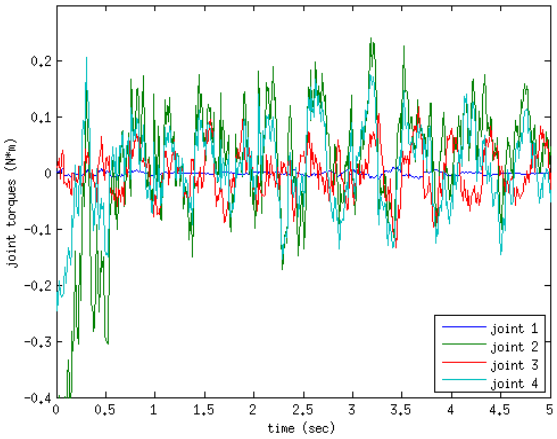

Figure 5: Joint torques commanded by the FMTJ controller in the presence of measurement noise ($\sigma = 0.15°$).

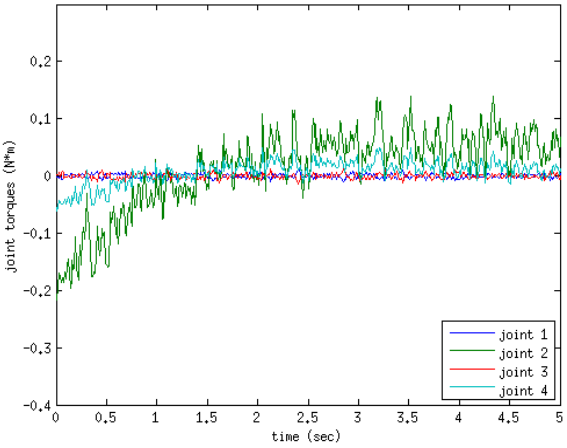

Figure 6: Joint torques commanded by the ID controller in the presence of measurement noise ($\sigma = 0.15°$).

	ϕ_{effort}	ϕ_{track}	Φ
TJ	58.40	7.80	66.20
MTJ	166.0	8.95	175.0
FMTJ	111.6	9.16	120.8
ID	1464	92.61	1557

Table 5: Controller performance in the presence of smaller knowledge errors ($\sigma = 0.038°$).

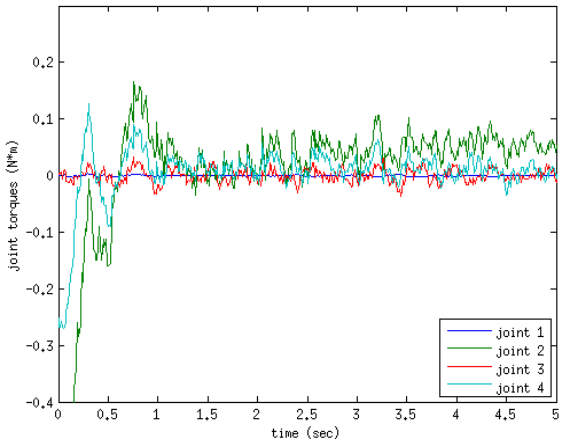

Figure 7: Joint torques commanded by the TJ controller in the presence of smaller measurement errors ($\sigma = 0.038°$).

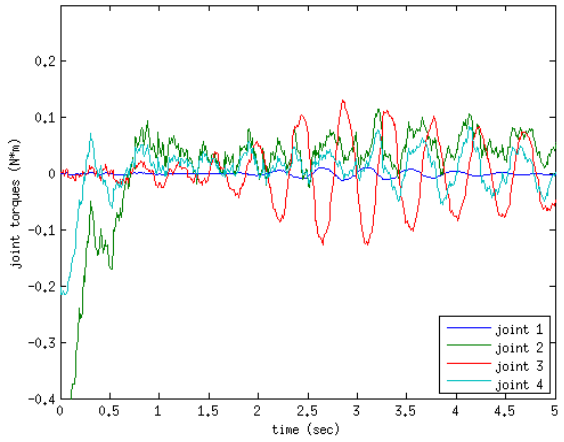

Figure 8: Joint torques commanded by the FMTJ controller in the presence of smaller measurement errors ($\sigma = 0.038°$).

VI. POSSIBLE ADAPTATION SCHEMES

The preceding discussion has assumed that all system parameters are precisely known, a condition which is impossible to achieve in practice. For this reason, it may be desirable to employ a system which can adaptively learn these parameters at runtime rather than depending on a nominal model. It is a goal of the DYMAFLEX project to test one or more such strategies as well. This section briefly outlines the nature of the problem and future work in this area.

For fixed-base manipulators, it is well known that the inertial and geometric parameters of the system can be linearly separated from functions of the joint angles vector $\underline{\theta}$ and its derivatives in the equations of motion [7]:

$$\mathbf{M}\dot{\underline{\nu}} + \underline{C} = \mathbf{Y}(\underline{\theta}, \underline{\nu}, \dot{\underline{\nu}})\underline{a}$$

where $\mathbf{Y}$ is the (known) regressor matrix containing the nonlinear functions of the system position and velocity states, and the vector $\underline{a}$ contains the uncertain system parameters. A typical adaptation law is then given by [6]:

$$\dot{\hat{\underline{a}}} = -\mathbf{\Gamma}^{-1}\mathbf{Y}^T\underline{r}$$

$$\underline{r} = \underline{\nu} - \underline{\nu}_{ref} + \mathbf{\Lambda}(\underline{\theta} - \underline{\theta}_{ref})$$

where $\hat{\underline{a}}$ is an estimate of the actual system parameters $\underline{a}$, $\mathbf{\Gamma}$ and $\mathbf{\Lambda}$ are positive-definite gain matrices, and $\underline{\theta}_{ref}$ and $\underline{\nu}_{ref}$ are reference joint angles and joint rates being commanded. Note that computation of $\mathbf{Y}$ requires knowledge of the system acceleration state, imposing additional sensing and/or filtering requirements versus the control strategies of the previous sections.

Vance [8] notes that this linear separability of the equations of motion is equally valid for a free-flying manipulator. Liang et al. [9] further present a formulation which allows for the same linear separability in the free-*floating* case, when RCS thrusters are not used. Despite the similarity in structure to the dynamics of a fixed-base manipulator, however, the fully-expanded symbolic expressions for the equations of motion of the DYMAFLEX system are extremely lengthy. Even if the tedious and error-prone symbolic manipulations were performed successfully, it is unclear whether the resulting expressions could be made sufficiently compact as to be evaluated within a controller update cycle. This remains a topic for further investigation. It is noteworthy, however, that Abiko and Hirzinger [10] have implemented this style of adaptation in simulation for a free-floating space manipulator in which only the grasped payload, rather than the entire system, has uncertain properties. It stands to reason that a grasped payload might be the most uncertain part of the system in a great many applications of practical interest, and the possibility of using DYMAFLEX in this manner will be explored in future simulations.

As an alternative to adapting to only a handful of uncertain parameters, a neural network can be used to build a map of the equations of motion. Whereas the linear regression technique assumes that the equations of motion are symbolically known and it

is simply the numerical values of some of these symbols which are uncertain, a neural network can approximate a general nonlinear function. Although this approach considerably increases memory requirements, its generic applicability is quite appealing, especially in the presence of unmodeled dynamics. Vance [8] presents a detailed analysis of such a control strategy for space manipulators, and it would be most interesting to test this strategy in the space environment.

VII. CONCLUSION

Preliminary simulation results have been presented comparing the performance of several controllers for the tracking of a desired trajectory in Cartesian space. An inverse dynamics strategy, canceling out the nonlinear behavior of the system, was found to require excessive control effort. The family of Transpose Jacobian strategies yielded adequate performance without feedback linearization. A technique was proposed for mitigating the control signal chattering of the Modified Transpose Jacobian controller, for which further investigation is necessary. It was shown that the MTJ and FMTJ strategies yield substantial improvements over the basic TJ approach in the idealized case. It was also shown, however, that the introduction of measurement noise can completely reverse this conclusion. This discrepancy underscores the limitations of any simulation-based analysis; and it is only through on-orbit testing that the practical capabilities of any space manipulator control scheme can be properly assessed. If chosen for flight, the DYMAFLEX system will test these and other controllers in the space environment to flight-validate these results. Future work prior to launch will attempt to assess robustness to uncertainty in the system parameters, the effects of unmodeled phenomena such as flexible modes and joint friction, and the feasibility of implementing adaptive control.

ACKNOWLEDGMENTS

The authors gratefully acknowledge the support of the United States Air Force Research Laboratory, whose funding via grant FA95501110046 has made this work possible under the University Nanosat Program 7 (UNP-7). Thanks are especially due to program coordinators David Voss, Amanda Pietruszewski, and Melody Ford, whose guidance, organizational effort, and general expertise have proven invaluable in the development process. Finally, the authors thank Dr. Craig Carignan, who contributed some of the computer code that was adapted for the present simulations.

REFERENCES

[1] K. McBryan and D. Akin. Mission overview of the dynamic manipulator flight experiment (DYMAFLEX): A nanosatellite test bed to study coupled dynamics between a robotic arm and an equivalently-sized small host vehicle in the space environment. In *63rd International Astronautical Congress*, 2012.

[2] E. Papadopoulos. *On the dynamics and control of space manipulators.* PhD thesis, Dept. of Mechanical Engineering, Massachusetts Institute of Technology, 1990.

[3] C. Carignan and D. Akin. The reaction stabilization of on-orbit robots. *IEEE Control Systems Magazine*, pages 19–33, December 2000.

[4] S. Moosavian and E. Papadopoulos. Control of space free-flyers using the Modified Transpose Jacobian algorithm. In *Proc. IROS*, pages 1500–1505, 1997.

[5] M. Karimi and S. Moosavian. Learning-based Modified Transpose Jacobian control of robotic manipulators. In *Proc. IEEE Conf. on Advanced Intelligent Mechatronics*, pages 1290–1295, 2008.

[6] M. Spong, S. Hutchinson, and M. Vidyasagar. Multivariable control. In *Robot modeling and control*, chapter 8, pages 289–318. Wiley, 2006.

[7] M. Spong, S. Hutchinson, and M. Vidyasagar. Dynamics. In *Robot modeling and control*, chapter 7, pages 239–288. Wiley, 2006.

[8] E. Vance. *Adaptive control of free-floating and free-flying robotic manipulators.* PhD thesis, Dept. of Aerospace Engineering, University of Maryland, 1998.

[9] B. Liang, Y. Xu, and M. Bergerman. Mapping a space manipulator to a dynamically equivalent manipulator. Technical Report CMU-RI-TR-96-33, Carnegie Mellon University, 1996.

[10] S. Abiko and G. Hirzinger. An adaptive control for a free-floating space robot by using inverted chain approach. In *Proc. IEEE/RSJ International Conference on Intelligent Robots and Systems*, pages 2236–2241, 2007.

IAC-12-D1.2.5

Ms. Katherine McBryan
University of Maryland, College Park, United States, kmcbryan@gmail.com

Dr. David L. Akin
University of Maryland, College Park, United States, dakin@ssl.umd.edu

MISSION OVERVIEW OF THE DYNAMIC MANIPULATOR FLIGHT EXPERIMENT (DYMAFLEX): A NANOSATELLITE TEST BED TO STUDY COUPLED DYNAMICS BETWEEN A ROBOTIC ARM AND AN EQUIVALENTLY-SIZED SMALL HOST VEHICLE IN THE SPACE ENVIRONMENT

Robotic arms have been proven to be extremely useful in the space environment. These manipulators have been fairly slow, with a tip velocity on the order of a few cm/s, and attached to large host vehicles to react the dynamics. These large host vehicles and manipulators are expensive, both in terms of development time and money. One of the design benefits of a slow moving arm on a large host vehicle is that the coupled dynamics are not an issue. Moving the arm at low speeds when attached to large host vehicle will result in small (and generally negligible) motions in the base vehicle. The dynamic manipulation flight experiment (DYMAFLEX) involves the design of two new components: a high performance 4DOF manipulator, capable of a tip speed in excess of 25 cm/s, and a small host vehicle capable of active stabilization using reaction wheels and cold gas thrusters. The relative mass between the spacecraft and manipulator is 5.3, whereas previous systems incorporating a robotic arm such as Orbital Express and ETS-VII have relative masses of 15 and 24, respectively. The effects of the coupled dynamics caused by DYMAFLEX's low relative mass and high tip speed are anticipated to be significant. The manipulator will perform a variety of trajectories; the dynamics will be recorded and transmitted by IMUs located throughout the spacecraft and a single IMU which will be located on the end-effector. Initial experiments will be done without any active stabilization, allowing the simulations to be verified. Cold gas thrusters will be used in addition to reaction wheels to actively stabilize the spacecraft. Cold gas thrusters are used to counter large moments caused by faster movements Being able to accommodate the coupled dynamics between a manipulator and similar-sized host vehicle will allow smaller, and thus cheaper, vehicles to be able to use high performance manipulators to perform tasks such as satellite servicing faster. This report will summarize the mission, subsystems, and initial results of the DYMAFLEX project.

I. INTRODUCTION

Satellite servicing has been a subject of much research and interest for decades. Satellite servicing offers a way to repair satellites on orbit. These repairs may include, but are not limited to, refueling, adding science components, upgrading computers and adding power systems. These repairs can keep a satellite from needing to be replaced. This can save the cost of a new satellite and keep desired orbits from becoming overcrowded. There have been numerous successful satellite servicing human missions utilizing Extra-Vehicular Activities (EVAs). NASA astronauts on STS 61, 82, 103, 109, and 125 successfully conducted repairs on the Hubble Space Telescope. These five EVA missions greatly increased the life and usefulness of the telescope. [1]

EVA time is limited due to the inherent risk to persons, and is expensive in terms of cost. Robotic manipulators have been used to assist EVA missions in order to reduce risk and time. The Shuttle Remote Manipulator System (SRMS), or Canadarm 1 was designed and used for satellite servicing. The SRMS was used in over 50 missions including the repairs to the Hubble Space Telescope. Astronauts used the SRMS to maneuver themselves around the Hubble Space Telescope. [2]

There are multiple manipulators in the International Space Station (ISS). These manipulators are used for handling payloads in addition to aiding in repairs. These manipulators include the Mobile Servicing System (MSS), better known by its primary component Canadarm2. The MSS includes a mobile base, and a manipulator called Space Station Remote Manipulator System (SSRMS) and the Special Purpose Dexterous Manipulator (SPDM or "Dextre"). The Japanese Experiment Module Remote Manipulator System (JEM-RMS) is also located on the ISS and primarily used to service the JEM exposed facility.[3] [4]

All manipulators require a control scheme. Accurate controlling of a manipulator's end-effector or tool tip is vital to satellite servicing as grasping another vehicle or an object is a vital part of satellite servicing. The canonical control laws were originally developed for fixed base manipulators and then adapted for space applications. Space manipulators, unlike fixed base manipulators, are mounted to a body which is able to rotate and move in reaction to the arm. The coupled dynamics increases the difficulty of accurately controlling a manipulator's end-effector.

A few mitigation strategies have been developed to control or reduce the coupled dynamics experienced by the base of the spacecraft. The ETS-VII mission described and experimentally demonstrated a zero-reaction maneuver. A manipulator with redundant degrees of freedom, such as 8DOF or 9DOF, can maneuver the redundant joints in such a way as to produce zero reaction to the base. A zero reaction maneuver is not always possible. This maneuver requires multiple redundant degrees of freedom. A 6 DOF manipulator is capable of performing a zero reaction maneuver in some select cases but not all. Much research has been done on path planning to minimize base reactions. [3]

Path planning can be used to reduce the base disturbances. The physical design of the manipulator and the vehicle it is mounted to can also affect the coupled dynamics. Faster moving and more massive manipulators result in greater coupled dynamics. In order to reduce this, space manipulators are often run at reduced speeds. The unloaded speed for the Canadarm2 is 37cm/s but the maximum loaded speed depends on the application. The tip speed during station assembly is 2 cm/s, while doing EVA support the maximum speed is 15 cm/s. Space manipulators are attached to large masses relative to their own mass. The Canadarm2 has a mass of 1800 kg, in comparison to the ISS which has a mass of approximately 420000 kg. [4], [5]

The Dynamic Manipulator Flight Experiment (DYMAFLEX) is a microsatellite with a high performance manipulator. The purpose of the vehicle is to investigate the coupled dynamics and associated control mitigation strategies for a free-flying vehicle performing tasks analogous to satellite servicing. The weight ratio between the arm and the vehicle is much less than previously flown experiments. In addition the manipulator will perform experiments at 25 cm/s, which is faster than a typical space manipulator maneuver. Presented is an overview of the DYMAFLEX system. Section II gives an overview of the mission plan and the experiments. Section III describes the subsystem of the vehicle and section IV concludes with future work.

II. MISSION OVERVIEW

The purpose of the DYMAFLEX mission is to investigate the coupled dynamics and associated control mitigation strategies for a free-flying vehicle with a high performance manipulator performing tasks analogous to satellite servicing. These analogous tasks include moving in Cartesian space, picking up masses and being able to compensate for the change in the systems' inertia, and use a thruster system in conjunction with the manipulator. The control strategies to be tested involve several non-adaptive methods as well as an adaptive one. The non-adaptive methods include a proportional differential (PD) controller, a passivity based controller, and an inverse dynamics based controller. An inertial measurement unit (IMU) is located in the manipulator tip. This IMU and three located in the base of the spacecraft will allow the control algorithms to be evaluated. Three IMUs are used for redundancy and to allow the signals to be filtered.

The second goal of the DYMAFLEX project is to develop a microsatellite in the university environment through a program which maximizes opportunities for students. Students are involved in all aspects of the development process. DYMAFLEX is being developed at the University of Maryland as part of the University Nanosatellite Program, sponsored by the Air Force Research Lab. Through this project, students at all university levels have been involved in developing the project. DYMAFLEX leverages three decades of advanced space robotics research done at the Space Systems Laboratory and the University of Maryland. This research focuses in the development and flight demonstration of a space manipulator system.

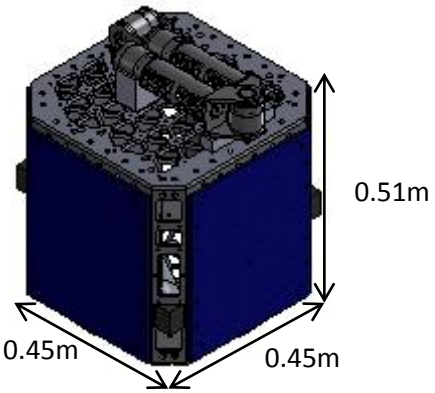

Figure 1: DYMAFLEX with manipulator in stowed configuration for launch

The DYMAFLEX project is a 50 kg microsatellite. The mass of the manipulator is approximately 7 kg. The major dimensions can be seen in Figure 1. The height of the base vehicle without the manipulator is approximately 0.4m.

i. Experiments

There are a number of planned experiments. The first set of experiments will be done once the manipulator is deployed. The shoulder joint will go through a sinusoidal movement for a few minutes under the control of each of the three non-adaptive control strategies. Three 9DOF IMUs located in the satellite will record the movement of the base. An IMU in the manipulator tip as well as absolute encoders will allow the position of the arm to be determined. The tip velocity will be 25 cm/s. These tests will be repeated with a 2DOF motion and a 3DOF motion.

The next set of experiments involves moving the manipulator in Cartesian space. This is more complicated, as the inverse kinematics must be solved in real time. Moving the manipulator in this way is done by moving the end-effector to a given Cartesian point. The controller must use inverse kinematics to determine what joint angles are necessary to achieve that end position. Joint limits and angular velocity limits must be taken into account. The Jacobian is used to relate the joint velocities and force to pose. This is necessary to drive the end effector along a desired Cartesian trajectory. This can become a problem as the manipulator approaches a singularity and the Jacobian cannot be inverted. This happens at the end of the work space and when two joints align, essentially causing the loss of a degree of freedom. Satellite servicing missions are done in Cartesian space, since the goal is to move the manipulator to the desired location in order to interact with other objects.

The third set of experiments involves using the thrusters in conjunction with arm motion. Thrusters can be used to control movement of the base of the spacecraft. A method of simplifying the control method would be to use the thrusters to keep the base stable and thus controlling the space manipulator like a fixed based manipulator. However, the life of most spacecraft is often limited by the amount of propellant on board; using the propellant to keep the base stable would severely limit the functional lifetime of the spacecraft. Instead of using the propellant to keep the base stable, the thrusters will be used with the manipulator in order to develop a control method that will control the base in conjunction with the manipulator.

The last part of the experiment makes use of tip masses. There are two tip masses located on the base vehicle. The manipulator is able to pick up the tip masses and perform the same maneuvers previously described. The control algorithms do not know the mass of the masses. This tests the sensitivity of the various control methods to the initial conditions, and also tests the adaptive controller's ability to adapt. Physical tip masses are used instead of changing a variable in the control algorithm because this allows the entire dynamics to change. Relocating a physical mass changes the inertia of the entire system, not just the mass of the manipulators tip.

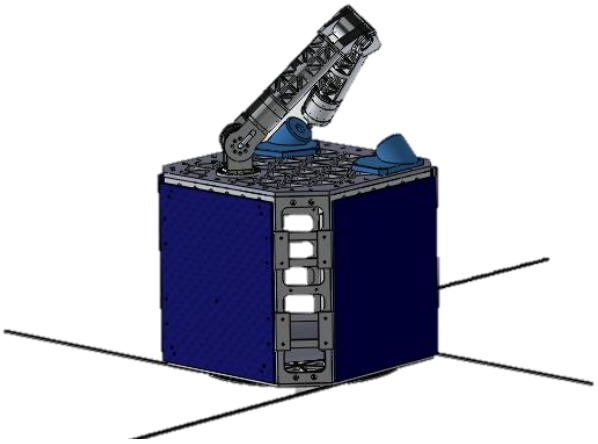

Figure 2: DYMAFLEX with the manipulator deployed. The manipulator does not have extra degrees of freedom in the tool-tip, so the tip masses must be designed based on geometry of the arm and where they are each mounted.

III. SPACECRAFT OVERVEIW

This section includes a brief description of the various components and subsystems on DYMAFLEX.

ii. Robotic Manipulator

The robotic manipulator is required to move in Cartesian space. The user can specify a point in X,Y, and Z space, within the manipulator reach, and the manipulator can move the tool tip to that location. This requires at least three joints in order to have the necessary degrees of freedom. This does not allow control of tip orientation in Cartesian space. For full 6DOF motion, at least six joints are required. DYMAFLEX has four degrees of freedom; while three DOF is required to allow end point positioning, the fourth joint aids in stowing the arm for launch. It also allows the manipulator to have one redundant degree of freedom, which can be used in path planning and to avoid singularities.

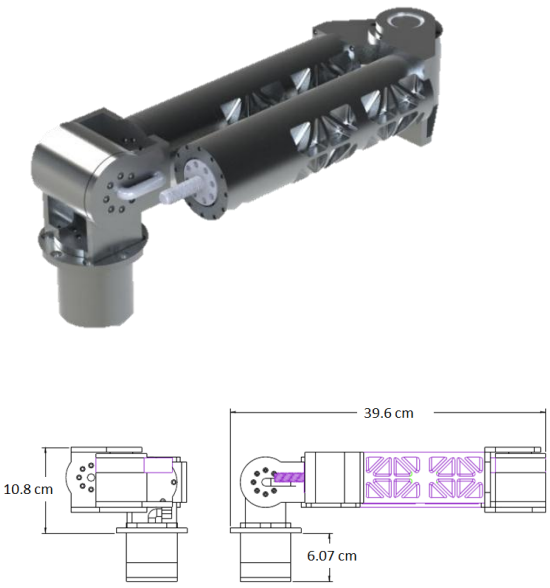

Figure 3: DYMAFLEX manipulator in the stowed configuration.

The DYMAFLEX arm consists of four revolute joints. Each joint has a brushless motor with a harmonic drive, a motor controller, a heater and temperature sensors. The manipulator is mounted outside the main spacecraft. It is expected that the manipulator, even with insulation, will require heaters at each joint in order to keep the motors and motor controllers from dropping below minimum survival temperatures while off. Temperature sensors are located in the joints to not only activate the heaters, but also to turn off the motors and the controllers should they become too hot.

The DYMAFLEX manipulator is designed to run most experiments at 25cm/s, which will provide significant coupled dynamics. The manipulator was also designed to run in Earth's gravity; this allows the manipulator to be tested on the ground without the use of a rigging system or a neutral buoyancy tank. The actuators are actually capable of a tip velocity in excess of 1 m/s, but will be restricted in software to the 25 cm/sec operating limit.

Figure 4: Manipulator in a deployed configuration

The DYMAFLEX manipulator is sized such that it is approximately 7 kg. This represents about 15% of the total mass of the vehicle. The two tip masses are 1 kg and 2 kg. Picking up the tip masses represents a significant increment in the manipulator mass. The manipulator is sized such that it cannot reach the bottom of the spacecraft, which is a program requirement to keep the satellite from interfering with the launch vehicle.

iii. Attitude Determination and Control System

The main part of the attitude determination system is the control algorithms previously described. These algorithms will be used to control the manipulator in desired motions. The motion will be measured by a 9DOF IMU located at the tip of the arm and three

located in the satellite base for redundancy. A Kalman filter will be used to filter the measurements from the three sensors. Every planned maneuver is on the order of a few minutes, generally less than five minutes. The IMU state estimate drift experienced during that time will be minimal.

Each maneuver can potentially leave the spacecraft tumbling. There are three hysteresis rods located on the spacecraft, mounted orthogonal to each other. These hysteresis rods are sized to dampen out the residual motion in one orbit. These rods are passive and should have little effect on the coupled dynamics during the manipulator maneuvers.

The ADCS typically includes the reaction control system (RCS). The thrusters, which make up the RCS system, are used to control the attitude of the spacecraft. It was determined that the ADCS and the RCS were both very large components of the DYMAFLEX project. The ADCS would be focused on the control methods while RCS would focus on the propulsion.

iv. Reaction Control System

The RCS consists of 16 cold gas thrusters. This allows full 6 degrees of freedom. Despite the fact that it is possible to translate, the thrusters will only be used to control orientation. There are four thruster quads located on the diagonals of the spacecraft. Each thruster quad is made up of four nozzles and four solenoids, one solenoid per nozzle.

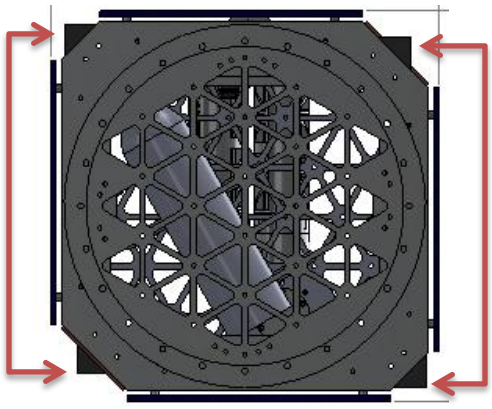

Figure 5: Location of thruster quads from top view

A study was done to determine the propellant type. This was based on a propellant that could produce 0.5 N of thrust per nozzle and minimize propellant mass and tank mass. This study compared carbon dioxide, nitrous oxide, and R134-A. These results were compared and CO_2 was selected. The performance difference between nitrous oxide and the carbon dioxide was shown to be negligible. R134-A does not have the same performance and is a poor choice of propellant for this project. CO_2 was then chosen based on safety concerns. The DYMAFLEX project is a student project and therefore safety is a major concern.

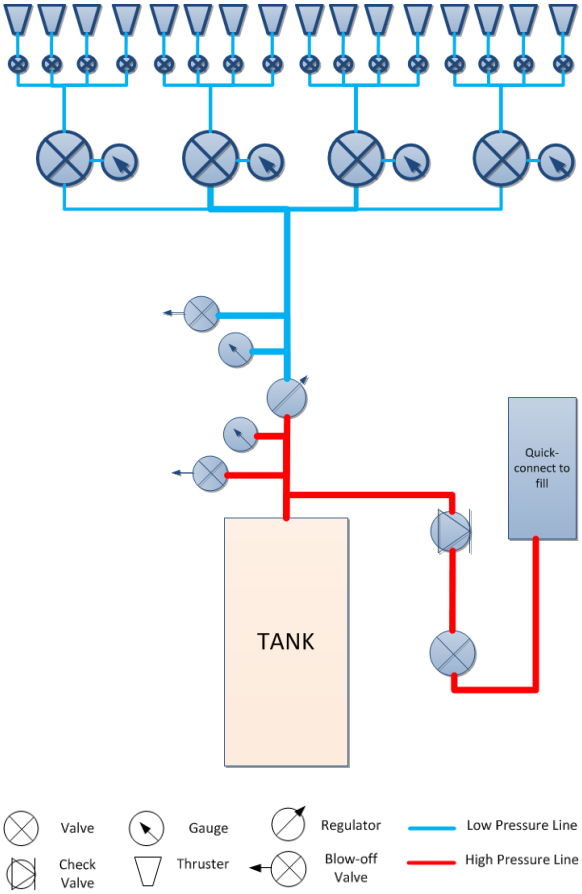

Figure 6: Block diagram of RCS

Reaction wheels were originally part of the DYMAFLEX design. Three reaction wheels each mounted perpendicular would aid in keeping the base stable without using propellant. The reaction wheels would aid in reorienting the vehicle after a movement. The reaction wheels were sized to output 10mNm of torque. This would not be enough to keep the base stable while the manipulator moved at 25 cm/s. The wheels would become saturated during such a movement. Due to cost and complexity the reaction wheels were removed from the DYMAFLEX mission.

v. Structures and Mechanisms

This system specialty consists of the design of the structure, ensuring the vehicle can survive launch, and developing the mechanism to restrain the manipulator during launch. The structure consists of an aluminum frame with aluminum housing for the subsystems. The electronics boxes are mounted onto isogrid frames, which are standardized in configuration and allow for a more modular design.

The isogrids have connecting members connecting them to the diagonal panels. This is to reduce vibrations as well as increase thermal paths. During assembly these connecting members will be hinged, which will aid in the assembly of the spacecraft. The hinges will allow the isogrid panels to open without removing fasteners. The wiring harness is designed to have service loops which will allow the subsystems to be serviced without removing any major parts. Before launch and during structural testing, the hinges will be replaced with connecting members.

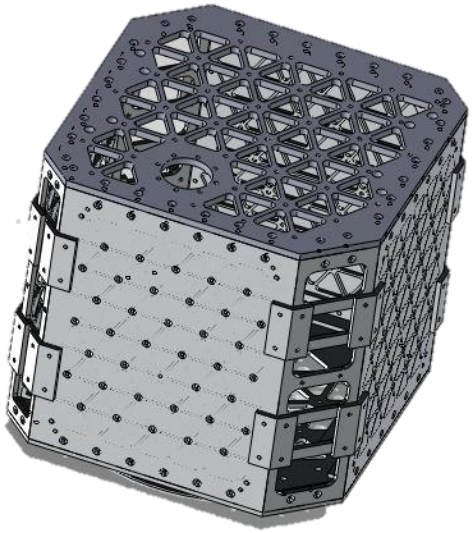

Figure 7: The main structure is made of Aluminum 6061-T6. The various side panels are connected to the top and bottom via brackets

The structures subsystem also handles mechanisms on DYMAFLEX including a restraint mechanism for the manipulator. The manipulator must be restrained during launch to prevent any harm from occurring to the launch vehicle or surrounding payloads. Non-pyrotechnic actuators will be used to hold the manipulator at the shoulder joint. In addition a mechanical rest is placed at the elbow to ensure the manipulator can survive the expected launch loads.

vi. Communications

The communications system consists of three radios, providing independent high and low bandwidth communications to a ground station. The low bandwidth consists of an ultra-high frequency (UHF) radio for downlink and very-high frequency (VHF) radio for uplink. Four half wave-length dipole antennas are located near the bottom of the satellite. These antennas will be deployed after separation from the launch vehicle. Since the manipulator cannot reach the bottom of the spacecraft, the antennas will be in no danger of getting hit should the manipulator become unstable.

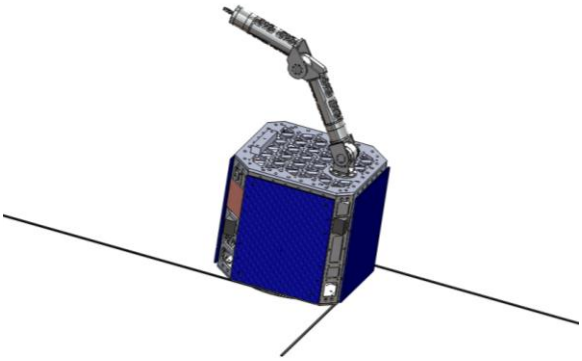

Figure 8: DYMAFLEX with antennas deployed

The low bandwidth radios were tested on a scientific balloon payload. The experiment was designed to track packet loss. A temperature sensor was used to record data and the radios were used to transmit. The system experienced about 3% packet loss. The payload was recovered after the flight.

The high bandwidth link uses an S-band transmitter. This radio is used for downlinking experimental data. The experimental data can be sent down via the low bandwidth antennas but would take multiple days to download all the data, whereas the S-band radio can transfer the data in a single day. There are two patch antennas located on the diagonals of the spacecraft. The use of multiple patch antennas reduces the pointing requirements necessary for communication.

vii. Electrical Power System

The electrical power system supplies power to the various subsystems. There are four solar panels, each one located on the isogrid panels. These four solar panels provide the power necessary to run the experiments and to keep the spacecraft alive. The panels provide enough power to directly run most subsystems when not in eclipse. This does not include the manipulator and the S-band radio.

The four solar panels are the same dimensions. A panel, when fully exposed at 90% illumination, is expected to produce 14.35 W. This was calculated with an assumed solar cell efficiency of 15%. The S-band transmitter and the manipulator are the major power draws; and during the states where these systems are on, there is a negative power budget. These systems are run for a very limited duration and must be turned on via a command from the ground.

The photovoltaic panels are used to charge nickel cadmium batteries. The batteries provide power during the experiment mode, when the manipulator is being used, during S-band communication and during eclipse. The manipulator will only be run when the batteries are charged. After each experiment, the batteries will need to recharge before proceeding to the next experiment.

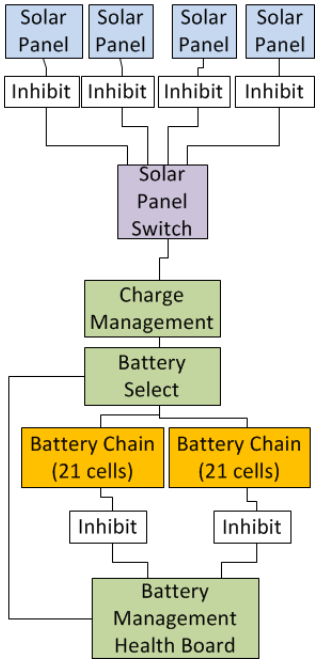

Figure 9: EPS block diagram

viii. Command and Data Handling

The command and data handling system consists of the main flight computer, control computer and how the various boards communicate with each other. The main flight computer major components are a microcontroller and an FPGA. The microcontroller is the main processor while the FPGA is used to connect to the various sensors and boards in the satellite.

There is also a control computer which can directly control the manipulator once the flight computer relinquishes control. The main flight computer can put the satellite into a safe state should the manipulator exceed specified limits. The control computer is only used during experiments.

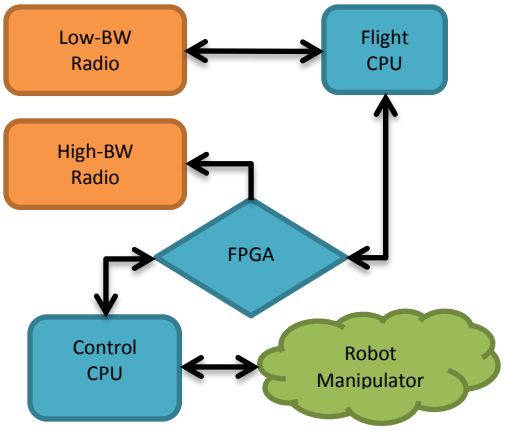

Figure 10: Block diagram of C&DH

A significant amount of design and developmental work has been completed. The DYMAFLEX project has entered the phase where the subsystems are being built and tested. A full "flatsat", non-flight configured version of the satellite's various boards, has been done with the prototype boards. A second flatsat is currently being built with the boards in the final form factor. Environmental testing is scheduled for later this year.

IV. CONCLUSIONS

DYMAFLEX is a student satellite designed to investigate the coupled dynamics between a satellite base and a high performance manipulator. DYMAFLEX will compare how various control methods are able to mitigate the coupled dynamics. These control methods include multiple non-adaptive methods as well as an adaptive method. Removable tip masses and a thruster system will be used to

further test the ability of the control algorithms to perform satellite servicing tasks.

Like all satellites, there are many different systems that need to function in order to meet the science goals. These systems include structures, electronics, software, communication, etc. Presented here is an overview of the various subsystems that are necessary for the DYMAFLEX to successfully complete the mission.

V. ACKNOWLEDGMENTS

The authors would like to thank our sponsors who have helped throughout our development of these systems: David Voss, Melody Ford, and Amanda Pietruszewski and the Air Force Research Lab, work conducted under grant FA95501110046.

The authors would also like to thank the students who have worked and continue to work on the DYMAFLEX project, especially the project leads.

Table 1: DYMAFLEX subsystems

Subsystem	Abbreviation /Acronym	Lead Engineer
Structures and Mechanisms	STRM	Katherine McBryan
Electrical Power Systems	EPS	Nicholas Limparis
Attitude Determination and Control System	ADCS	Nicholas D'Amore
Reaction Control System	RCS	Katherine Strickland
Communications	COMMS	Constance Ciarleglio
Command and Data Handling	C&DH	Nicholas Limparis
Robotic Manipulator	ROBO	Christopher Carlsen
Thermal	THRM	Katherine McBryan
Software	SOFT	Kit Sczudlo

VI. REFERENCES

[1] "NASA Hubble Space Telescope," 11 July 2012. [Online]. Available: http://www.nasa.gov/mission_pages/hubble/servicing/index.html. [Accessed August 2012].

[2] "Canadarm," 09 08 2012. [Online]. Available: http://www.asc-csa.gc.ca/eng/canadarm/default.asp. [Accessed August 2012].

[3] "Space Station Assembly," NASA, 23 Oct 2010. [Online]. Available: http://www.nasa.gov/mission_pages/station/structure/elements/jem.html. [Accessed Sept. 2012].

[4] "Space Station Assembly," NASA, 23 Oct 2012. [Online]. Available: http://www.nasa.gov/mission_pages/station/structure/elements/mss.html. [Accessed Sept 2012].

[5] J. Wu, S. Shi, B. Wang, Z. Jiang and H. Liu, "Path planning for minimizing base reaction of space robot and its ground experimental study," in *IEEE International Conference on Mechatronics and Automation*, Changchun, China, 2009.

[6] "Canadarm and Canadarm2 - Comparative table," 31 12 2002. [Online]. Available: http://www.asc-csa.gc.ca/eng/iss/canadarm2/c1-c2.asp. [Accessed 10 Sept 2012].

[7] "Facts and Figures," 25 July 2012. [Online]. Available: http://www.nasa.gov/mission_pages/station/main/onthestation/facts_and_figures.html. [Accessed 11 Sept. 2012].